Chemical Engineering Journal Advances 12 (2022) 100387

Contents lists available at ScienceDirect

Chemical Engineering Journal Advances

journal homepage: www.sciencedirect.com/journal/chemical-engineering-journal-advances

Nitrate removal in saline water by photo-reduction using natural $FeTiO_3$ as catalyst

Jefferson E. Silveira [a,b,c,*], Alicia L. Garcia-Costa [a], Jaime Carbajo [a], Alyson R. Ribeiro [b], Gema Pliego [a], Wendel S. Paz [c,*], Juan A. Zazo [a], Jose A. Casas [a]

[a] Department of Chemical Engineering, Universidad Autónoma de Madrid, Cantoblanco, Madrid, 28049 Spain
[b] Department of Preventive Veterinary Medicine, Veterinary School, Federal University of Minas Gerais, Minas Gerais, 31270-901, Brazil
[c] Departamento de Física, Universidade Federal do Espírito Santo, Vitória, ES 29075-910, Brazil

ARTICLE INFO

Keywords:
Nitrate
Photo-reduction
Brackish groundwater
Ilmenite
Water conditioning

ABSTRACT

As climate change progresses, there is an increasing interest on the use of non-conventional water sources such as brackish or saline waters. Nowadays, the main threat in Europe detected in these waterbodies is nitrate contamination. Within the multiple available methods studied for nitrate reduction, photocatalysis presents promising results, but this technology has not yet been tested in saline water. This work tackles the elimination of nitrate ($[NO_3^-]$ =50 mg/L) in brackish and saline water ([sea salt] = 5–33 g/L) using ilmenite as photocatalyst and oxalic acid as an environmental-friendly reducing agent. The main challenge when working in saline water is to overcome oxalic acid scavenging by Ca^{2+} present in the water matrix. This can be solved either working at over stoichiometric concentrations of oxalic acid (≈300% stoich. dose) or acidifying the reaction media. The addition of hydrochloric acid ensures the protonation of oxalic acid, reducing drastically its precipitation as CaC_2O_4. Working at $[C_2O_4^{2-}]$ = 180 mg/L, $[FeTiO_3]$ = 450 mg/L and [HCl 37%] = 13 mM, 73% total nitrogen (TN) elimination was reached after 420 min. Reaction temperature was also evaluated in the range of 20–80 °C, which allowed to calculate the E_a=9.8 kJ/mol. Finally, the effect of dissolved O_2 on the TN reduction was assessed. Overall, photocatalytic nitrate reduction presents itself as a feasible technology regardless of the water salinity.

1. Introduction

The intense use of fertilizers and agrochemicals is still a generalized practice in agriculture, leading to a negative environmental fingerprint. As reported by the European Commission [1], nitrate-based fertilizers are the most employed in Europe. Nitrogenated compounds are essential for vegetal production but, after addition, their excess may reach the water bodies through processes such as run-off and leaching. The improper disposal of animal waste and aquaculture effluents is also an important entry of nitrogen into the aquatic environment [2]. Nitrate pollution has impacted several water bodies worldwide, increasing the pressure on already polluted sites and fragile areas as coastal, arid, and semiarid regions.

The nitrate pollution issue is regulated both by the European Union [3] as well as locally by the Spanish public administration [4]. Complementarily, control actions have been made, as the delimitation of Nitrate Vulnerable Zones (NVZ) and the establishment of Codes of Good Agricultural Practices. However, a 2019 report shows that around 46% of Spanish groundwater bodies presented nitrate pollution [1]. The same was observed recently in monitoring sites across Europe, where the average nitrate concentration of many fresh and saline groundwater samples surpassed the threshold of 50 mg/L [5]. Nowadays, the scientific focus is directed towards the treatment of contaminated freshwater, ignoring the fact that salinity and nitrate pollution may occur together. A remarkable example of such mixed scenario is the *Mar Menor* (Murcia, Southeast of Spain) case. Being one of Europe's biggest saline lagoons with approximately 17.000 hectares, this touristic coastal water body is surrounded by an overexploited agricultural region with an intense use of nitrogenated fertilizers, and some old mining areas. Furthermore, it is located over the brackish and chronically polluted *Campo de Cartagena* aquifer [6–8]. Like other aquifers, *Campo de Cartagena* presents different layers, each one of them affected by different anthropogenic processes as intense groundwater exploitation, agricultural nutrients permeation and seawater intrusion. Ions as Na^+, Mg^{2+}, Ca^+ and $Cl^-$from saltwater

* Corresponding authors.
E-mail addresses: jefferson.silveira@uam.es (J.E. Silveira), wendel.paz@ufes.br (W.S. Paz).

https://doi.org/10.1016/j.ceja.2022.100387
Received 25 May 2022; Received in revised form 16 August 2022; Accepted 24 August 2022
Available online 31 August 2022

intrusion contribute to the contamination of unconfined aquifers. To allow its use in irrigation, desalination of groundwater via reverse osmosis (RO) has been used in this region for decades, producing rejected brine with high nitrate and other ions concentrations, that is posteriorly disposed in the lagoon [7,8] which leads to a huge growth of algae. Also, during torrential raining, the runoff of old mining waste disposed in nearby creeks and agrochemicals residues may sum up to the lagoon contamination. Geomorphological peculiarities of coastal lagoons as sediment formation and hindered waves make them singular and fragile water bodies [6,9]. As a result, eutrophication episodes with high mortality of aquatic organisms have been constantly reported in *the Mar Menor*. The nutritional disbalance caused by multifactor pollution promotes an intense phytoplankton growth in the epipelagic zone, that hinders light transmittance through the water body, compromising the viability of mesopelagic and lower communities [9].

Over the last decades, different treatments, including biological [10,11] and physical-chemical approaches [12–14] have been proposed to remove nitrates from surface and groundwater. Industrial facilities for nitrate removal are mainly based on reverse osmosis and ion exchange processes [15]. However, these are physical processes that merely transfer the pollutant from a diluted stream to a concentrated one, which needs to be further treated.

Alternatively, catalytic reduction processes have been studied at lab scale. These include catalytic and photocatalytic nitrate reduction. Catalytic nitrate reduction has been widely explored, employing noble metals (Pd, Pt, Ru, Rh) as active phase in heterogeneous catalysts [16]. So far, this process presents a fast nitrate depletion. Still, it has not been implemented at industrial scale due to NH_4^+ formation along the process, which compromises the quality of the effluents. This drawback can be overcome with photocatalytic nitrate reduction employing the adequate photocatalyst. Prior studies of our group demonstrate the efficiency of ilmenite ($FeTiO_3$) as a natural, low-cost photocatalyst in nitrate reduction [17]. Moreover, our process is based on the use of oxalic acid as an environmentally-friendly electron donor. This reducing agent is ultimately transformed into CO_2, while NO_3^- undergo subsequent reduction stages to $NO_3^- \rightarrow NO_{2\,(g)} \rightarrow NO_2^- \rightarrow NO_{(g)} \rightarrow N_2O \rightarrow N_{2\,(g)}$. The use of ilmenite as photocatalyst is particularly interesting in this process, as the conduction band of this material is located below the hydrogen reduction potential, hindering the water splitting photo-reaction and avoiding the NH_4^+ production. So far, this technology has been applied to both ultrapure water and real groundwater intended for human consumption, hence, with a low salinity.

In this work, nitrate reduction in saline waters is explored for the first time employing the $FeTiO_3$/oxalic acid photocatalytic process. The performance of this process is analyzed in the context of groundwater affected by seawater intrusion and nitrate pollution, including operational feasibility as temperature effects.

2. Material and methods

2.1. Chemicals and reactants

Sea salt was provided by Instant Ocean, USA. Sodium nitrate (99%), oxalic acid dihydrate ($\geq$ 99%), and hydrochloric acid (37%) were purchased from Sigma-Aldrich, USA. N_2 (g) was supplied by Praxair S.L. Ilmenite ($FeTiO_3$, Ref. 50,110,700) was provided by Marphil S.L. (Spain) and employed without further treatment. The main physical-chemical properties, as well as further characterization parameters from the employed ilmenite are available elsewhere [18]. In brief, this mineral presents an Fe and Ti content of 36.2% and 37%, respectively, with a very low specific area (S_{BET}: 6 m^2/g), pH_{slurry}: 8.4, a 2.4 eV band-gap and a slight magnetic behavior (M_S: 0.19 emu/g) (see Fig. S1a-S1c as Supplementary material).

Table 1
Sea salt composition and 33 g/L SSW characterization.

	Sea salt (%)	33 g/L SSW (mg/L)
TC	–	32.6
TOC	–	n.d
TIC	–	32.6
HCO_3^-	0.6	200
Cl^-	57.6	19,000
SO_4^{2-}	8.2	2700
Na^+	27.2	8980
K^+	1.3	420
Ca^{2+}	1.2	400
Mg^{2+}	3.9	1300

2.2. Photocatalytic experiments

The system set-up consisted of a magnetically stirred sealed glass jacketed batch reactor (700 mL useful volume). A 150 W medium mercury lamp (TQ150 Heraeus), with 30 W/cm^2 irradiance, was placed at the center of the reactor (Fig S2). The UV–Vis irradiation has been directly measured by a photoradiometer (Delta Ohm, model HD 2102.1). The characteristic UV spectrum given by the manufacturer is provided in the Supporting Information (Fig. S3)

The concentration of oxalic acid was varied between one and three times the stoichiometric amount needed for complete reduction of NO_3^- to N_2 (3.6 g $C_2O_4^{2-}$ / g NO_3^-).

Synthetic seawater (SSW) was prepared by dissolving the corresponding amount of sea salt in ultrapure water to achieve initial salt concentration amid 5 and 33 g/L. Full characterization of sea salt and the 33 g/L synthetic seawater can be found in Table 1.

Additionally, control tests without sea salt with various water matrix constituents (HCO_3^-, Ca^{2+}, Mg^{2+}, K^+, SO_4^{2-}, Cl^-) were also carried out in parallel. Temperature was varied in the range 20–80 °C using a recirculating water bath (Huber). The ilmenite concentration was kept at 450 mg /L. When not stated otherwise, continuous N_2 flow of 370 mL/min was employed to maintain the reaction system under inert conditions. All experiments were performed in triplicate.

2.3. Analytical methodology

Oxalic acid decomposition and total nitrogen reduction were followed by measuring total organic carbon (TOC) and total nitrogen (TN), respectively, using a TOC-L with TNM analyzer (Shimadzu).

3. Results and discussion

3.1. Initial runs

As may be seen, SSW presents neither dissolved organic matter nor NO_3^-, but it shows a complex composition with a wide variety of anions and cations. In order to test nitrate photo-reduction in SSW, this was spiked with [NO_3^-] = 50 mg/L which corresponds to a total nitrogen (TN) concentration of 11.8 mg/L. Nitrate photo-reduction requires the addition of oxalic acid as reducing agent, as depicted in Eqs (1)-3 [19]:

$$NO_3^- + 5e^- + 6H^+ \rightarrow 1/2 N_{2\,(g)} + 3\,H_2O \quad (1)$$

$$C_2O_4^{2-} \rightarrow 2\,e^- + 2\,CO_2 \quad (2)$$

$$NO_3^- + 5/2\,C_2O_4^{2-} + 6\,H^+ \rightarrow 1/2\,N_{2\,(g)} + 3\,H_2O + 5\,CO_2 \quad (3)$$

When introducing the stoichiometric dose required for complete 50 mg/L nitrate reduction ([$C_2O_4^{2-}$] = 180 mg/L), there was a noticeable increase in the water turbidity, as can be seen in Figure S4a of the Supporting Information (SI). The high Ca^{2+} concentration in the water matrix, as shown in Table 1, causes a quick calcium oxalate precipitation. This results in around a loss of 30% of the reducing agent as well as

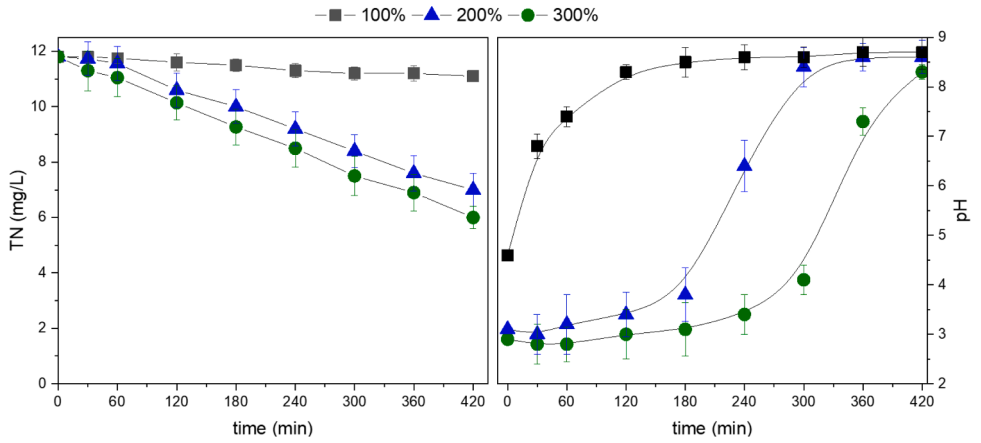

Fig. 1. NO_3^- photo-reduction in saline water, a) TN and b) pH evolution. Operating conditions: $[FeTiO_3]_0$ = 450 mg/L, $[C_2O_4^{2-}]_0$ = 100–300% stoichiometric dose, 180–540 mg/L, [sea salt] = 33 g/L, T = 20 °C, N_2 = 370 mL/min.

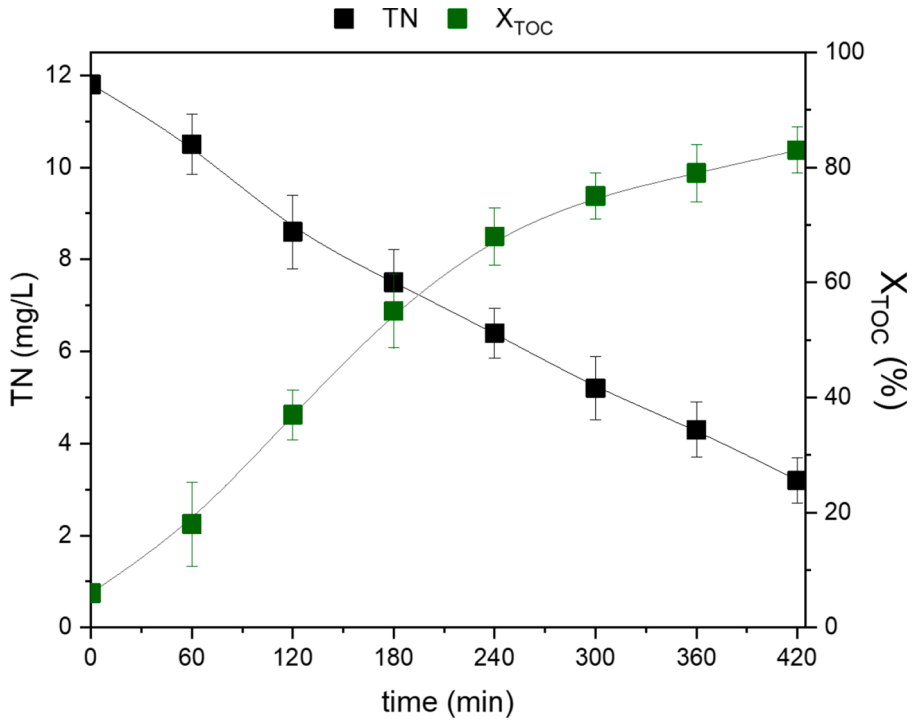

Fig.. 2. NO_3^- photo-reduction in saline water. Effect of initial acidification using HCl on TN photoreduction. Operating conditions: $[FeTiO_3]_0$ = 450 m/L, $[C_2O_4^{2-}]_0$ = 100%, $[NO_3^-]$ = 50 mg/L, T = 20 °C, [sea salt] = 33 g/L, HCl= 13 mM, N_2 = 370 mL/min.

the increase of the turbidity. Consequently, the process efficiency is highly diminished (Fig. 1). To overcome the oxalic acid scavenging, NO_3^- photo-reduction was tested as well with 200% and 300% of the stoichiometric dose of oxalate, which corresponds to $[C_2O_4^{2-}]$ = 360 mg/L and 540 mg/L, respectively. Increasing the reducing agent dose by two-fold, a 47% of the nitrogen content is eliminated. Nonetheless, higher doses did not have a significant effect on the N removal rate.

Besides, according to Fig. 1b, the pH value steeply increases at the beginning of the reaction, probably due to the H^+ consumption by bicarbonate or sulfate. Therefore, the availability of the two main reagents needed for NO_3^- reduction, H^+ and $C_2O_4^{2-}$ (Eq. (3)), is limited.

In Fig. S5, control experiments in a null salinity condition in the presence of typical water ions (HCO_3^-, Ca^{2+}, Mg^{2+}, K^+, SO_4^{2-}, Cl^-) were performed to check natural matrix effects on N_2 selectivity. In the case of calcium, its role is related to oxalate precipitation. On the other hand, our findings indicate that bicarbonate has the largest effect on the energy barrier, favoring the adsorption of OH^- instead of NO_3^- and NO_2^- adsorptions at the ilmenite surface. The contribution of the other ions showed a negligible effect in the N_2 selectivity [20].

Aiming to minimize these drawbacks, HCl was added to the reaction media at 13 mM. In these conditions, CaC_2O_4 production is not favored, resulting in a transparent reaction media as shown in Fig. S4b. Maintaining the pH below 3, both oxalic acid and H^+ availability is ensured, resulting in an effective TN reduction, as seen in Fig. 2. The HCl run presented a stable pH value between 2.5 – 3, well below the pH_{slurry} of ilmenite, favoring the oxalic acid decomposition and TN depletion. The overall performance of the process, as shown in Fig 2. is still below the stoichiometry of the denitrification reaction, probably due to the competition with other species in parasitic reactions. However, TN removal is increased from 8% to 73% under the same operating conditions when adding HCl to the reaction media. Therefore, subsequent experiments were performed with HCl addition.

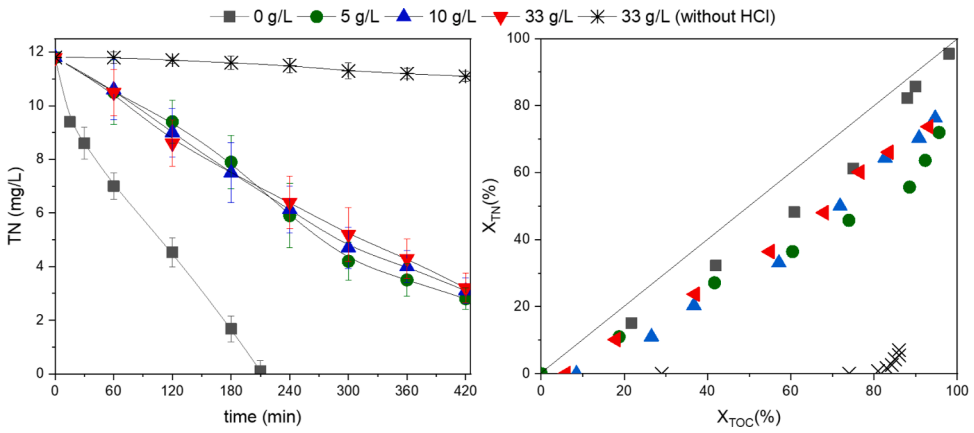

Fig.. 3. Effect of salinity on nitrate photo-reduction **a**) TN evolution and **b**) reductant exploitation. Operating conditions: $[FeTiO_3]_0$ = 450 mg/L, $[C_2O_4^{2-}]_0$ = 180 mg/L, $[NO_3^-]$ = 50 mg/L, T = 20 °C, [sea salt] = 5–33 g/L, HCl: 13 mM.

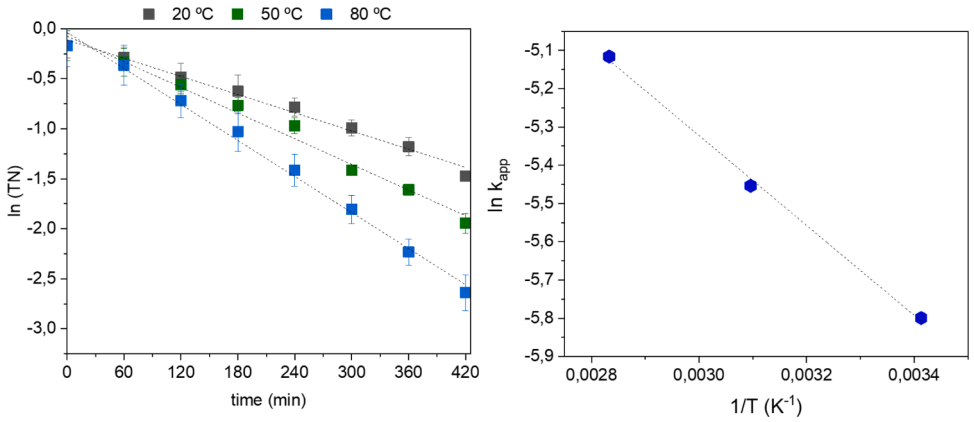

Fig. 4. Effect of temperature on nitrate photo-reduction **a**) Total Nitrogen`s pseudo-first kinetic order fit, **b**) Arrhenius plot. Experimental conditions: $[FeTiO_3]_0$ = 450 m/L, $[C_2O_4^{2-}]_0$ = 180 mg/L, $[NO_3^-]$ = 50 mg/L, T = 20 −80 °C, [sea salt] = 33 g/L, HCl = 13 mM, N_2 = 370 mL/min.

3.2. Effect of water salinity on nitrate photoreduction

Aiming to determine the efficiency of the process in a wider range of salinity for its application in brackish groundwater bodies, nitrate photo-reduction was addressed working at 5, 10 and 33 g/L sea salt concentrations, maintaining the HCl acidification, $FeTiO_3$ at 450 mg/L and using the stoichiometric dose of oxalic acid. For the sake of comparison, the TN evolution in a null salinity matrix (miliQ) and in a 33 g/L water without HCl addition, were also included (Fig. 3). In all these experiments, the pH remains well below 3, despite the increase in the HCO_3^- concentration. It should be noted that in all saline – pH controlled runs, the TN evolution showed a similar trend.

Furthermore, the reducing agent exploitation was analyzed in Fig. 3b. As the oxalic acid dose applied corresponds to the stoichiometric dose for complete nitrate reduction towards $N_{2(g)}$, the ideal behavior of the system would correspond to the diagonal, where each fraction of oxalic acid consumed (X_{TOC}), is employed to eliminate the same fraction of nitrogenated species in solution (X_{TN}). This ideal behavior takes place in a simple matrix using ultrapure water. However, using 33 g/L saline aqueous matrix without adding HCl, the experimental data fall well below the diagonal, meaning that most of the electrons obtained from the oxalic acid oxidation, or oxalic acid itself, are interacting with other inorganic species, mainly Ca^{2+} and HCO_3^- [19]. The acidification with HCl allows to partially overcome this dramatically reduction on X_{TN} / X_{TOC} ratio (up to around 80%), as HCO_3^- is removed and CaC_2O_4 precipitation is avoided, regardless of the water salinity within the studied range.

Table 2
Apparent first order rate constants for nitrate photo-reduction at 20–80 °C.

Operating temperature (°C)	$k_{app}\cdot10^3$(min^{-1})	r^2
20	3.03 ± 0.14	0.994
50	4.28 ± 0.22	0.993
80	6.00 ± 0.21	0.996

The effect of initial nitrogen concentration was also investigated, working at 50 and 150 mg/L NO_3^-. As shown in Fig. S6, the photocatalytic activity was moderately inhibited as initial NO_3^- increased (maintaining the same catalyst dose), with the extent of TN reduction decreasing from 74 to 65% after 420 min, and the corresponding k_{app} decreasing from 3.03 to 2.23 $0{\cdot}10^3$ min^{-1}, at 50 and 150 mg/L NO_3^-, respectively. This could be explained by the passivation of the $FeTiO_3$ surfaces as increasing anions/$FeTiO_3$ ratio [19].

3.3. Effect of temperature on nitrate photoreduction

Groundwater treatment only makes sense in ambient conditions. Nonetheless, during photo-reduction experiments, if no temperature control is applied, the lamps heat the reaction media up to 50 °C. Hence, the effect of the temperature on nitrate photo-reduction was studied in the range of 20–80 °C, as shown in Fig. 4. As expected, an increase in the temperature is translated in enhanced reaction kinetics. The apparent kinetic constants (k_{app}) for the pseudo-first order fitting employed are collected in Table 2. With the obtained k_{app}, the activation energy was

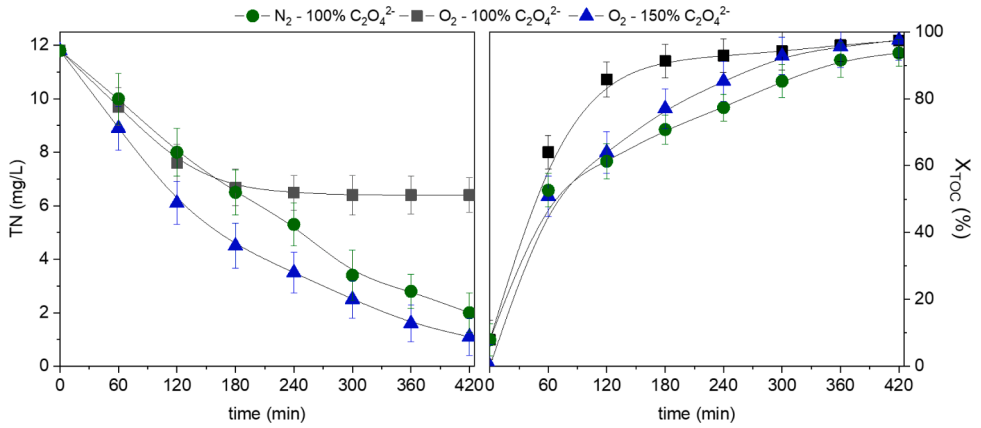

Fig.. 5. Effect of oxidative conditions and oxalic acid dose on nitrate photo-reduction **a**) TN evolution, **b**) TOC conversion. Experimental conditions: $[FeTiO_3]_0$ = 450 m/L, $[C_2O_4^{2-}]_0$ = 180 – 270 mg/L, $[NO_3^-]$ = 50 mg/L, T = 50 °C, [sea salt] = 33 g/L, HCl = 13 mM, N_2= 0 or 370 mL/min.

estimated (Fig. 4b) at E_a=9.8 kJ/mol. This value is significantly lower than those reported in the literature for catalytic hydrogenation using Pd-Cu bimetallic catalysts (E_a=47 kJ/mol) [20] Pd on carbon fibers (E_a=26 kJ/mol) [21] or Mg/Cu nanoparticles (E_a=14.2 kJ/mol) [22]. Thus, the proposed process not only employs a low-cost and highly available mineral as catalyst, but it lowers the energy requirements for the effective nitrate reduction in comparison to the most widely studied processes.

3.4. *Effect of dissolved oxygen on nitrate photoreduction*

Generally, photo-reduction reactions are carried out in an inert atmosphere (N_2) to avoid the competition of dissolved O_2 and NO_3^- for their reduction using electrons promoted to the conduction band. Since the increase of temperature, besides increasing the reaction kinetics, diminishes the oxygen solubility, working at 50 °C could make the process feasible without the need of an inert gas flow to remove O_2 in solution. Fig. 5 collects the results obtained at 50 °C using 100% and 150% of the stoichiometric oxalic acid dose. At 100% the stoichiometric dose, the effect of oxygen is more noticeable from t = 180 min onwards. At this point complete oxalic acid oxidation is reached, as seen in Fig. 5b, hindering the remaining TN reduction. This suggests that the dissolved O_2 at the beginning of the reaction acts as electron scavenger generating $O_2^{\bullet-}$, in acidic media this is quickly transformed into $HOO^{\bullet}$, taking H^+ from the reaction media. Without organic matter in the matrix, these $HOO^{\bullet}$ react amongst themselves yielding H_2O_2 and O_2, being the hydrogen peroxide ultimately eliminated as $H_2O + O_2$. Thus, there is a poor $C_2O_4^{2-}$ exploitation that results in a limited TN reduction. Still, a slight increase in the oxalic acid concentration to 150% of the stoichiometric dose results in a 91.5% TN elimination. Hence, despite the negative effect of dissolved O_2, both the increase in temperature and reducing agent help mitigate this effect, broadening the feasibility of the photo-reduction process towards its implementation at larger scale.

4. Conclusions

Saline water containing nitrates can be effectively treated by means of photocatalytic reduction using ilmenite as photocatalyst and oxalic acid as hole scavenger. Acidic pH values must be maintained to avoid oxalic acid precipitation by Ca^{2+} present in the water matrix. Under those conditions and compared to ultrapure water, salinity (in the range 5–33 g/L) has a small influence upon the nitrate reduction, which is related the evolution of $C_2O_4^{2-}$ concentration. Nevertheless, the reaction time was higher in comparison to the results reported in ultrapure water. Increasing the temperature accelerates the reaction, and it could also avoid the need of bubbling N_2 to maintain inert conditions. Thus, working at 50 °C and acidic pH, the total nitrogen conversion was well above 0.9 when using 1.5 times the stoichiometric $C_2O_4^{2-}$ dose without bubbling N_2 gas.

Funding information

This work has been supported by MICINN through the project PID2019–106884GB-I00 and Comunidad de Madrid through the project P2018/EMT-4341. J. Carbajo wants to thank the Ministerio de Ciencia, Innovación y Universidades (MICIU) for a grant under the Juan de la Cierva_Incorporación program (IJCI-2017–32,682). Jefferson E. Silveira gratefully acknowledge the support from CAPES: Science Without Borders Program, Ministry of Education Brazil, under grant BEX-1046/13–6. Alicia L. Garcia-Costa thanks the Universidad Autónoma de Madrid for the concession of a María Zambrano postdoc internship.

Declaration of Competing Interest

The authors declare that they have no known competing financial interests or personal relationships that could have appeared to influence the work reported in this paper.

Acknowledgements

This work has been supported by MICINN through the project PID2019–106884GB-I00 and Comunidad de Madrid through the project P2018/EMT-4341. J. Carbajo wants to thank the Ministerio de Ciencia, Innovación y Universidades (MICIU) for a grant under the Juan de la Cierva_Incorporación program (IJCI-2017–32682). Jefferson E. Silveira gratefully acknowledge the support from CAPES: Science Without Borders Program, Ministry of Education Brazil, under grant BEX-1046/13–6. Alicia L. Garcia-Costa thanks the Universidad Autónoma de Madrid for the concession of a María Zambrano postdoc internship.

Supplementary materials

Supplementary material associated with this article can be found, in the online version, at doi:10.1016/j.ceja.2022.100387.

References

[1] COM 257 final, Report from the commission to the council and the European parliament, Brussels 4.5 (2018).
[2] Parlamento Europeo, Directiva 2006/118/CE del Parlamento Europeo y del Consejo Europeo, 27/12/2006 2006 (2006) 13.
[3] EC, Protection of water against pollution caused by nitrates from agricultural sources, Off. J. Eur. Communities. L 269 (2000) 1–15.
[4] M.D.E.L.A. Presidencia, Boletín oficial del estado, (2022) 5664–5684.

[5] E. Abascal, L. Gómez-Coma, I. Ortiz, A. Ortiz, Global diagnosis of nitrate pollution in groundwater and review of removal technologies, Sci. Total Environ. 810 (2022), 152233.
[6] H.M. Conesa, F.J. Jiménez-Cárceles, The Mar Menor lagoon (SE Spain): a singular natural ecosystem threatened by human activities, Mar. Pollut. Bull. 54 (2007) 839–849, https://doi.org/10.1016/j.marpolbul.2007.05.007.
[7] B. Maxwell, C. Díaz-García, J.J. Martínez-Sánchez, J. Álvarez-Rogel, Increased brine concentration increases nitrate reduction rates in batch woodchip bioreactors treating brine from desalination, Desalination 495 (2020), 114629, https://doi.org/10.1016/j.desal.2020.114629.
[8] C. Puertes, I. Bautista, A. Lidón, F. Francés, Best management practices scenario analysis to reduce agricultural nitrogen loads and sediment yield to the semiarid Mar Menor coastal lagoon (Spain), Agric. Syst. 188 (2021), https://doi.org/10.1016/j.agsy.2020.103029.
[9] J. Álvarez-Rogel, G.G. Barberá, B. Maxwell, M. Guerrero-Brotons, C. Díaz-García, J. J. Martínez-Sánchez, A. Sallent, J. Martínez-Ródenas, M.N. González-Alcaraz, F. J. Jiménez-Cárceles, C. Tercero, R. Gómez, The case of Mar Menor eutrophication: state of the art and description of tested nature-based solutions, Ecol. Eng. 158 (2020), 106086, https://doi.org/10.1016/j.ecoleng.2020.106086.
[10] H. Chen, S. Liu, T. Liu, Z. Yuan, J. Guo, Efficient nitrate removal from synthetic groundwater via in situ utilization of short-chain fatty acids from methane bioconversion, Chem. Eng. J. 393 (2020), 124594, https://doi.org/10.1016/j.cej.2020.124594.
[11] X. Liu, M. Huang, S. Bao, W. Tang, T. Fang, Nitrate removal from low carbon-to-nitrogen ratio wastewater by combining iron-based chemical reduction and autotrophic denitrification, Bioresour. Technol. 301 (2020), 122731, https://doi.org/10.1016/j.biortech.2019.122731.
[12] S. Tyagi, D. Rawtani, N. Khatri, M. Tharmavaram, Strategies for nitrate removal from aqueous environment using nanotechnology: a review, J. Water Process Eng. 21 (2018) 84–95, https://doi.org/10.1016/j.jwpe.2017.12.005.
[13] M. Stjepanović, N. Velić, A. Lončarić, D. Gašo-Sokač, V. Bušić, M. Habuda-Stanić, Adsorptive removal of nitrate from wastewater using modified lignocellulosic waste material, J. Mol. Liq. 285 (2019) 535–544, https://doi.org/10.1016/j.molliq.2019.04.105.
[14] S. Duan, T. Tong, S. Zheng, X. Zhang, S. Li, Achieving low-cost, highly selective nitrate removal with standard anion exchange resin by tuning recycled brine composition, Water Res. 173 (2020), 115571, https://doi.org/10.1016/j.watres.2020.115571.
[15] E. Science, Review of the technologies for nitrates removal from water intended for human consumption review of the technologies for nitrates removal from water intended for human consumption, (n.d.). 10.1088/1755-1315/664/1/012024. 2020.
[16] H.O.N. Tugaoen, S. Garcia-Segura, K. Hristovski, P. Westerhoff, Challenges in photocatalytic reduction of nitrate as a water treatment technology, Sci. Total Environ. 599–600 (2017) 1524–1551, https://doi.org/10.1016/j.scitotenv.2017.04.238.
[17] J.A. Zazo, P. García-muñoz, G. Pliego, E. Silveira, P. Ja, J.A. Casas, Selective reduction of nitrate to N2 using ilmenite as a low cost photo- catalyst, Appl. Catal. B. 273 (2020) 1–6, https://doi.org/10.1016/j.apcatb.2020.118930.
[18] J.E. Silveira, W.S. Paz, P. Garcia-Muñoz, J.A. Zazo, J.A. Casas, UV-LED/ilmenite/persulfate for azo dye mineralization: the role of sulfate in the catalyst deactivation, Appl. Catal. B Environ. 219 (2017) 314–321, https://doi.org/10.1016/j.apcatb.2017.07.072.
[19] J.E. Silveira, A.R. Ribeiro, J. Carbajo, G. Pliego, J.A. Zazo, J.A. Casas, The photocatalytic reduction of NO3− to N2 with ilmenite (FeTiO3): effects of groundwater matrix, Water Res. 200 (2021), 117250, https://doi.org/10.1016/j.watres.2021.117250.
[20] A. Pintar, J. Batista, J. Levec, T. Kajiuchi, Kinetics of the catalytic liquid-phase hydrogenation of aqueous nitrate solutions, Appl. Catal. B Environ. 11 (1996) 81–98, https://doi.org/10.1016/S0926-3373(96)00036-7.
[21] V. Höller, K. Rådevik, I. Yuranov, L. Kiwi-Minsker, A. Renken, Reduction of nitrite-ions in water over Pd-supported on structured fibrous materials, Appl. Catal. B Environ. 32 (2001) 143–150, https://doi.org/10.1016/S0926-3373(01)00139-4.
[22] S.B. Mortazavi, B. Ramavandi, G. Moussavi, Chemical reduction kinetics of nitrate in aqueous solution by Mg/Cu bimetallic particles, Environ. Technol. 32 (2011) 251–260, https://doi.org/10.1080/09593330.2010.495399.